USGS Award Number G09AP00121

Final technical report: Predicting void redistribution-induced strength loss in liquefied soil

Principal Investigator:

Ross W. Boulanger, Ph.D., P.E.
University of California at Davis
Department of Civil and Environmental Engineering
One Shields Avenue
Davis, CA 95616

Phone (530) 752-2947
Email rwboulanger@ucdavis.edu

Award term:
July 2009 – June 2010

Research supported by the U.S. Geological Survey (USGS), Department of the Interior, under USGS award number (G09AP00121). The views and conclusions contained in this document are those of the authors and should not be interpreted as necessarily representing the official policies, either expressed or implied, of the U.S. Government.

Predicting void redistribution-induced strength loss in liquefied soil

Abstract

Estimating the residual shear strength (S_r) of potentially liquefiable soil continues to be one of the most uncertain steps in the evaluation of liquefaction-induced ground failure hazards for a wide range of civil infrastructure and lifeline facilities. The S_r of a liquefied soil can be strongly affected by void redistribution, in which lower permeability layers capping outward seepage driven by earthquake-induced pore-pressures cause significant loosening of some zones in the liquefied soil, thus leading to dramatically reduced shear strengths in those loosened areas. Physical modeling and numerical modeling studies have shown that the effects of void redistribution on shear resistances and deformations in liquefiable soils are highly dependent on all the factors that affect the generation and dissipation of earthquake-induced excess pore water pressures; e.g., soil mechanical properties (initial relative density, cyclic strength, compressibility), geometry (slopes and stratigraphy), permeability (magnitudes and contrasts), and earthquake loading characteristics (intensity, duration, and frequency content). Empirical interpretations of case history experiences are, unfortunately, insufficiently detailed to distinguish between field conditions that have the potential to lead to significant void redistribution-induced strength loss or not.

The present study evaluated the ability of a nonlinear dynamic modeling procedure to differentiate between the conditions under which void redistribution will or will not lead to significant strength loss or shear localization in the field. The nonlinear dynamic simulations were performed using the commercial program FLAC (Itasca 2009, 2011) with the user-defined constitutive model PM4Sand (Boulanger 2010, Boulanger and Ziotopoulou 2012). The critical state compatible framework of the PM4Sand model enabled direct simulation of void redistribution mechanisms. First, simulations at the element scale were used to explore the effects of partial drainage on the monotonic, cyclic, and post-cyclic behavior of liquefied sand. Single element simulations were shown to be capable of approximating published laboratory test data involving strength loss and deformations under partially drained loading conditions. The calibrated single element simulation models were then used to illustrate the effects of partial drainage on material responses under a broader range of cyclic and post-cyclic loading conditions (details in Kamai and Boulanger 2012). The nonlinear dynamic modeling procedure was then evaluated for its ability to approximate the recorded responses of dynamic centrifuge models influenced to various degrees by void redistribution. The simulation models were shown to be capable of reasonably approximating the range of recorded responses of centrifuge models involving the lateral spreading of a clay crust over a liquefied sand layer, with and without treatment by geo-synthetic drain elements (details in Boulanger et al. 2011 and Kamai and Boulanger 2011, 2013). Simulation results were also shown to reasonably approximate key features of the localized deformation mechanisms observed in a centrifuge model involving silt seams embedded in a slope of loose, saturated sand, although certain aspects of the recorded response remained difficult to reproduce (details in Boulanger et al. 2013, 2014). Current limitations in our ability to account for void redistribution effects in simulations and how they relate to current design practice for estimating residual shear strengths for liquefied soils were discussed in Boulanger et al. (2014).

Predicting void redistribution-induced strength loss in liquefied soil

1. Introduction

Estimating the residual shear strength (S_r) of potentially liquefiable soil continues to be one of the most important and uncertain steps in the evaluation of liquefaction-induced ground failure hazards for a wide range of civil infrastructure and lifeline facilities. The estimated strength dominates the design approach and can result in decisions regarding tens of millions of dollars in remediation costs for any single structure.

The residual shear strength of a liquefied soil can be strongly affected by void redistribution (NRC 1985; Whitman 1985), in which lower permeability layers capping the outward seepage and dissipation of earthquake-induced pore-pressures cause significant loosening of some zones in the liquefied soil, thus leading to dramatically reduced shear strengths in those loosened areas (Mechanism B in Figure 1). Physical modeling (shake table and centrifuge; e.g., Kokusho 2003, Kulasingam et al. 2004) and numerical modeling studies (e.g., Naesgaard et al. 2006; Seid-Karbasi and Byrne 2007) have shown that the effects of void redistribution on shear resistances and deformations in liquefiable soils are highly dependent on all the factors that affect the generation and dissipation of earthquake-induced excess pore water pressures; e.g., soil mechanical properties (initial relative density, cyclic strength, compressibility), geometry (slopes and stratigraphy), permeability (magnitudes and contrasts), and earthquake loading characteristics (intensity, duration, and frequency content). Empirical interpretations of case history experiences are, however, unable to distinguish between field conditions that have the potential to lead to significant void redistribution-induced strength loss or not, and thus do not provide a rational basis for estimating the post-liquefaction shear strengths of sands with corrected SPT $(N_1)_{60}$ values in the range of 15 to 25 (i.e., a situation commonly encountered in practice but which falls outside the range of the case history data).

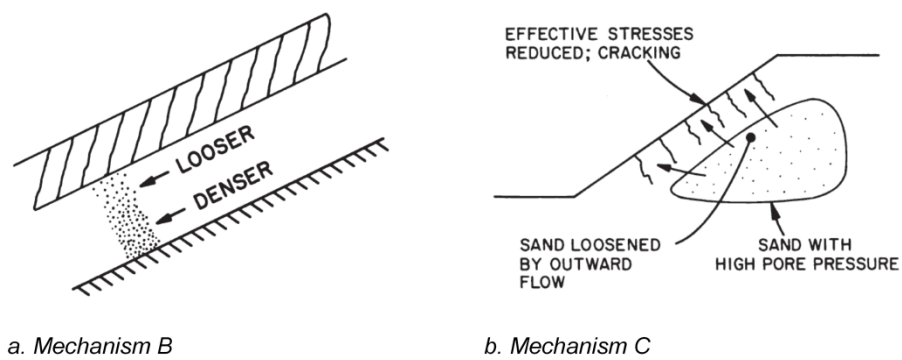

Figure 1. (a) Example of a potential situation for mechanism B failure arising from the rearrangement of the soil into looser and denser zones. Local volume change occurs, but the sand as a whole remains at a constant volume and is 'globally' undrained. (b) Example of a potential situation for mechanism C failure resulting from the migration of pore pressure into the overlying cohesive soils, thus reducing their shear resistance. This mechanism can be associated with global volume changes, cracks, and sand boils through the overlying crust layer. [Whitman 1985, NRC 1985].

The present study evaluated the ability of a nonlinear dynamic modeling procedure to differentiate between the conditions under which void redistribution will or will not lead to significant strength loss or shear localization in the field. The nonlinear dynamic simulations were performed using the commercial program FLAC (Itasca 2009, 2011) with the user-defined constitutive model PM4Sand (Boulanger 2010, Boulanger

and Ziotopoulou 2012, 2013). A critical state compatible framework, such as incorporated in the PM4Sand model, is a necessary feature for directly simulating void redistribution mechanisms. First, simulations at the element scale were used to explore the effects of partial drainage on the monotonic, cyclic, and post-cyclic behavior of liquefied sand. Single element simulations were compared to published laboratory test data involving strength loss and deformations under partially drained loading conditions. The calibrated single element simulation models were then used to illustrate the effects of partial drainage on material responses under a broader range of cyclic and post-cyclic loading conditions. The nonlinear dynamic modeling procedure was then evaluated for its ability to approximate the recorded responses of dynamic centrifuge models influenced to various degrees by void redistribution. The simulation models were shown to be capable of reasonably approximating the range of recorded responses of centrifuge models involving the lateral spreading of a clay crust over a liquefied sand layer, with and without treatment by geo-synthetic drain elements. Simulation results were also shown to reasonably approximate key features of the localized deformation mechanisms observed in a centrifuge model involving silt seams embedded in a slope of loose, saturated sand, although certain aspects of the recorded response remained difficult to reproduce. Current limitations in our ability to account for void redistribution effects in simulations and how they relate to current design practice for estimating residual shear strengths for liquefied soils were discussed. The following sections of this report summarize the above work and provide references for additional details.

2. Single-Element Simulations of Partial Drainage Effects

The first task, the results of which are reported in Kamai and Boulanger (2012), was to explore two questions related to the effects of partial drainage conditions on the monotonic, cyclic, and post-cyclic behavior of sands at the element scale. The first question is whether a constitutive model that has been shown to work reasonably well for fully drained or undrained laboratory element tests will also work reasonably well for a range of partially drained loading conditions. Addressing this question is a prudent step when using a constitutive model for problems affected by void redistribution processes; it was addressed in this work for the critical state-based constitutive model, PM4Sand. The model was first calibrated using data from drained and undrained lab tests on Toyoura sand (e.g., Figure 2). Then, single-element simulations, using the calibrated model and the program FLAC, were then compared to partially drained lab test data for Toyoura sand and to trends observed for other sands. The second question is how might partially drained loading conditions affect the behavior of sand to conditions not yet examined by laboratory element testing; e.g., how would partial drainage affect the cyclic resistance ratio and subsequent accumulation of shear strains for dense-of-critical sand that exhibits cyclic mobility behavior in fully undrained cyclic loading? Simulations were used to explore this latter loading condition, and the results were discussed relative to those that might reasonably be expected pending experimental confirmation. The importance of liquefaction-induced seepage and void redistribution to the in-situ strength and deformation behavior of liquefied sands was discussed in view of the results of these partially-drained laboratory element tests and simulations.

The PM4Sand model, after calibration to results of traditional drained and undrained tests on Toyoura sand, was able to reasonably predict the response of this sand to volumetric-strain-controlled, constant shear stress, monotonic injection tests (Sento et al. 2004), as shown in Figure 3, and predict responses consistent with those of Fraser River sand in constant volumetric-to-shear strain ratio monotonic injection tests (Vaid and Eliadorani 1998, 2000). The detrimental effect of an increasing volumetric-to-shear strain ratio on shear resistance is illustrated in Figure 4 for sand at the same initial relative density but subjected to different volumetric-to-shear strain ratios; a sufficiently high ratio can cause a sand to transition from shear-strain-hardening to shear-strain-softening behavior. The ability of the model to approximate the response of sand to these partially-drained loading conditions is primarily attributed to the reasonableness of its critical state framework and dilatancy relationship.

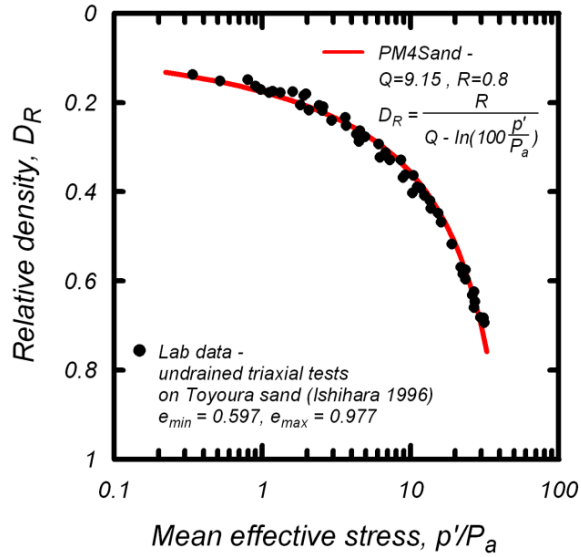

Figure 2. Critical-state line for Toyoura sand (Ishihara 1996) and the calibrated fit with PM4Sand by Kamai and Boulanger (2012).

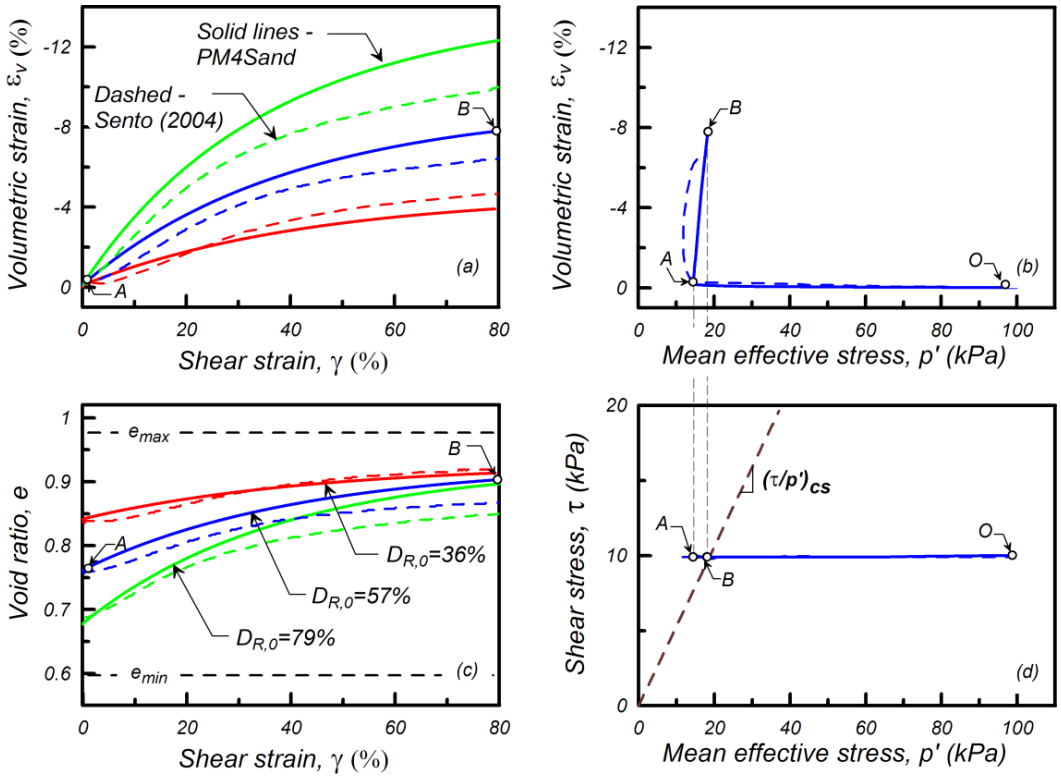

Figure 3. Comparison of volumetric strain controlled, constant shear stress lab tests, represented by the dashed lines (Sento et al. 2004) with simulations using PM4Sand, represented by the solid lines (Kamai and Boulanger 2012).

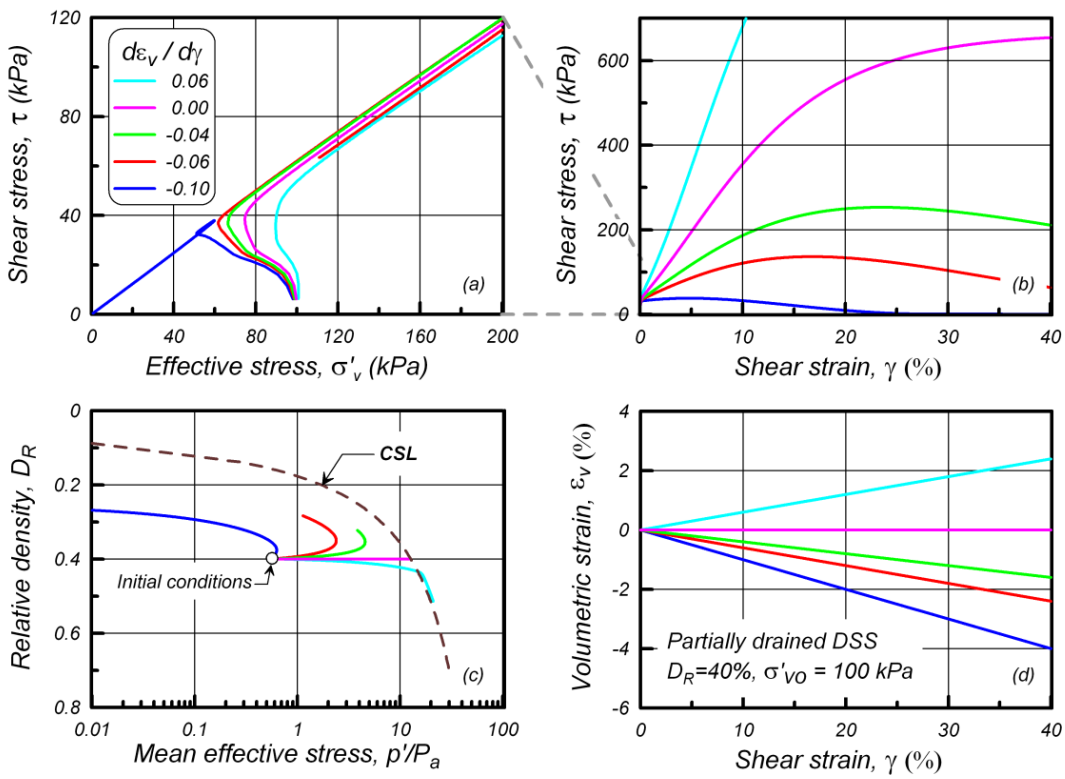

Figure 4. Results of constant volumetric-to-shear strain ratio simulations – showing undrained (ratio=0), expansion (negative ratio) and contraction (positive ratio) ratios - all for D_R=40%, and σ'_{v0}=100 kPa (Kamai and Boulanger 2012).

Results for the partially-drained, monotonic and cyclic loading conditions examined indicated that the detrimental effects of water injection decrease as a sand becomes more dense-of-critical. Sands with greater initial relative densities have greater dilatancy and thus greater capacity to 'absorb' the imposed volumetric strains with less loss of strength and/or smaller deformation. The results also show, however, that a relatively modest injection rate or injection volume can cause large strains and/or strength loss in sands that are only slightly dense of critical.

For field conditions, the detrimental effects of liquefaction-induced void redistribution can be expected to decrease even more rapidly with increasing relative density because the volume of water expelled by the re-consolidating portions of a liquefied sand layer will also progressively decrease with increasing relative density (Ishihara and Yoshimine 1992). This expectation is consistent with the fact that post-shaking flow deformations or water film formation in physical model tests have been largely limited to models with relatively loose sands and well-defined low-permeability inter-layers (Kokusho 2003, Kulasingam et al. 2004).

The results of this task, as summarized in Kamai and Boulanger (2012) provided a basis for understanding the behavior of sand elements in larger boundary-value simulations, such as the centrifuge test simulations described in the following sections.

3. Simulations of Dynamic Centrifuge Model Tests

Nonlinear dynamic simulations were performed for two dynamic centrifuge model tests which were influenced to different degrees by void redistribution. The first centrifuge test involved lateral spreading of a clay crust over a liquefied sand layer, with and without treatment by geo-synthetic drain elements. The other centrifuge test involved a slope of loose, saturated sand with embedded silt seams which exhibited post-shaking deformations due to void redistribution. The results of these simulations are briefly summarized below.

3.1 Lateral spreading of clay crust over liquefied sand with and without drains

The first set of simulations, which are reported in Kamai and Boulanger (2013), was for a centrifuge model which consisted of two mild slopes separated by a channel in the middle, as shown in Figure 5. One slope was treated with geo-synthetic drains and one was not. The simulations were performed using the mesh shown in Figure 6. Calibration of the constitutive model PM4Sand is illustrated by the simulated modulus reduction and damping relationships shown in Figure 7 and the cyclic resistance ratios summarized in Figure 8. Additional details of the calibration process are provided in Kamai (2011) and Boulanger and Ziotopoulou (2012).

Simulations were conducted for four successive shaking events, using two cyclic strengths that bound the laboratory strength data (Figure 7). Comparisons of the simulation and centrifuge results are used to address the following questions: (1) Can the simulation successfully capture key mechanisms and features? (2) Can the simulation successfully capture the trend and magnitude of results? (3) How sensitive are the results to some of the uncertain parameters? (4) What additional insight can be gained from the numerical simulation that could not be obtained directly from the physical test?

On average, results from the individually-run simulations and the in-sequence simulations yield comparable results in terms of the dynamic response and final deformations. Differences in results between these two approaches are mostly evident in the cumulative effects of void redistribution, with the in-sequence simulations better illustrating the progressive loosening of sand immediately beneath the overlying clay crust.

The general trends that were observed in the centrifuge test are successfully captured in the numerical simulations of all four shaking events. Simulations with ‘Case A’ and ‘Case B’ estimates of cyclic strength for the loose sand provide a reasonable bound on the measured responses (e.g., Figures 9, 10, and 11). The simulation with 1/3 of the lab-based estimate of permeability provided better agreement with the dissipation rates observed in the centrifuge test but did not improve the predictions of lateral displacements for that scenario. The simulation without pore fluid flow did not predict the dissipation patterns and redistribution of densities that were observed in the test and thus under-estimated the lateral displacements. Accounting for mesh geometry updating (large deformation effects) was essential for obtaining reasonable simulation results. The progressive flattening of the ground surface, especially due to the rotational movement of the slope in shake 10, had a significant effect on restraining the accumulation of deformations; thus allowing the mesh geometry to update during shaking enabled the simulations to account for the progressive changes in crust slope.

The processes of pore pressure dissipation and void redistribution that were observed on the non-treated side in the centrifuge test were reasonably simulated for all shaking events (Figures 11 and 12). The sequential simulations were more successful in capturing the cumulative effect of loosening in the upper portion of the sand layer such that the final amount of volumetric strain and the thickness of the loosening

zone were consistent with previous studies of this centrifuge test and others (Malvick et al. 2006, Kamai and Boulanger 2010). The location and magnitude of deformations that developed across the shear band were only partly captured by the simulations and were largely underestimated, illustrating an important limitation of currently available simulation models.

The benefits of the drains on the treated side of the centrifuge model were reasonably approximated in the numerical simulations; including effectively mitigating the surface displacements and preventing the concentration of shear strains. These simulations assumed perfect drainage walls, however, which would be expected to result in an over-estimation of their beneficial effects.

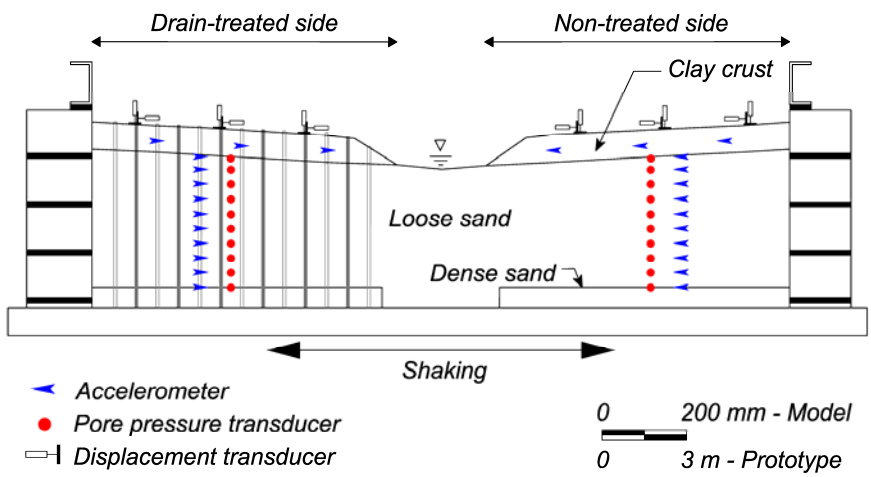

Figure 5. Schematic representation of the centrifuge test layout (Some instruments are omitted for clarity) (Kamai and Boulanger 2013).

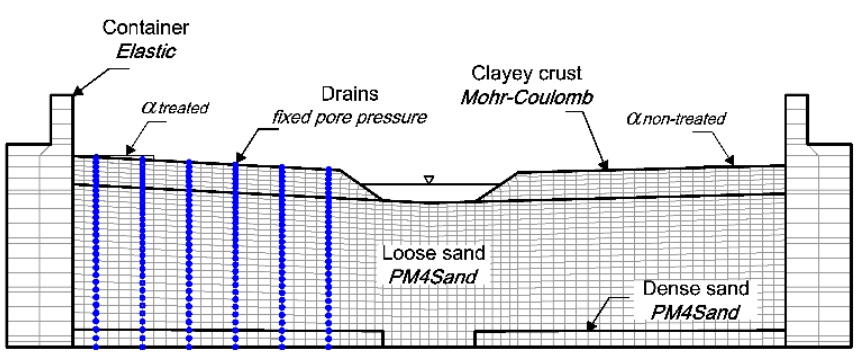

Figure 6. FLAC mesh, showing location of drains and water table height. For the individually-run simulations, slope angle was defined separately in each shake for the treated and non-treated sides, as denoted by $\alpha_{treated}$ and $\alpha_{non\text{-}treated}$. (Kamai and Boulanger 2013)

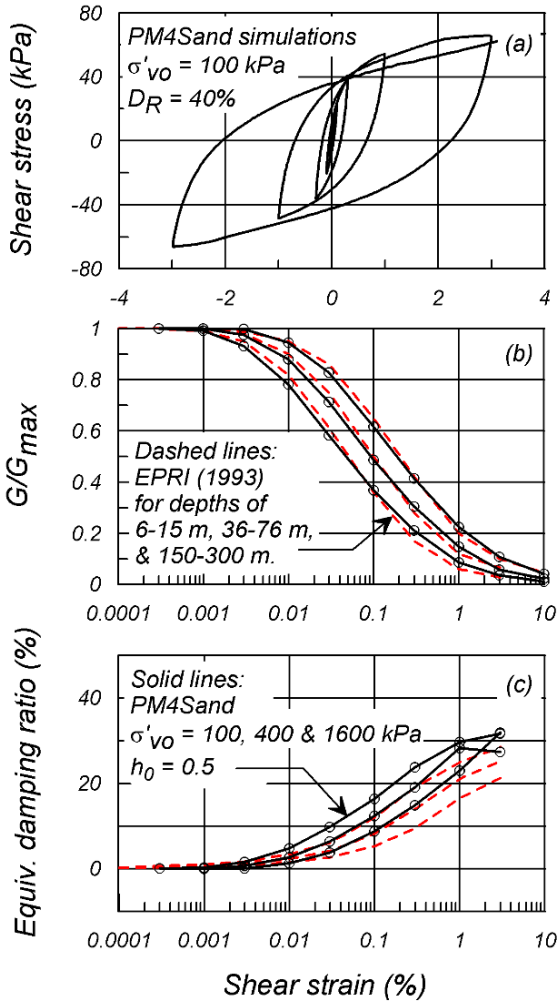

Figure 7. Modulus degradation and damping ratio curves, comparing simulation results in solid lines with empirical design relationships for sand in dashed lines (EPRI 1993). (a) Drained, cyclic DSS single-element simulation (b) strain-dependent modulus degradation at different confinement levels (c) strain-dependent damping ratio at different confinement levels. (Kamai and Boulanger 2013)

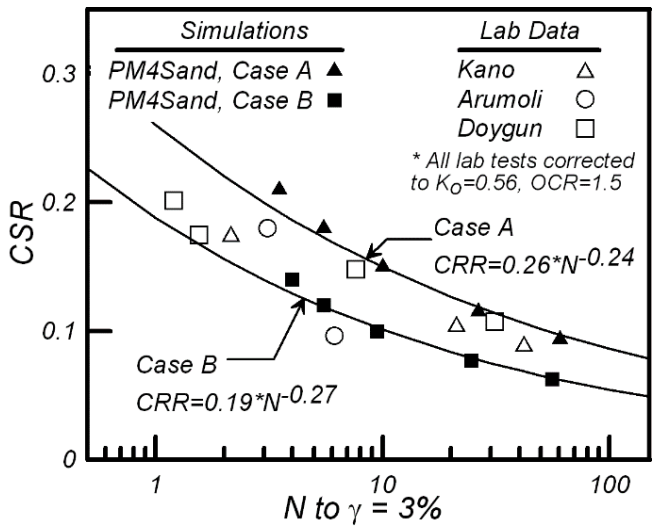

Figure 8. Triggering calibration for *PM4Sand* – number of cycles required to reach 3% shear strain under constant cyclic stress ratio (CSR). Lab data for loose Nevada Sand is shown in open symbols, calibrated simulation results shown in full symbols. The two curves represent a power fit to the data. (Kamai and Boulanger 2013)

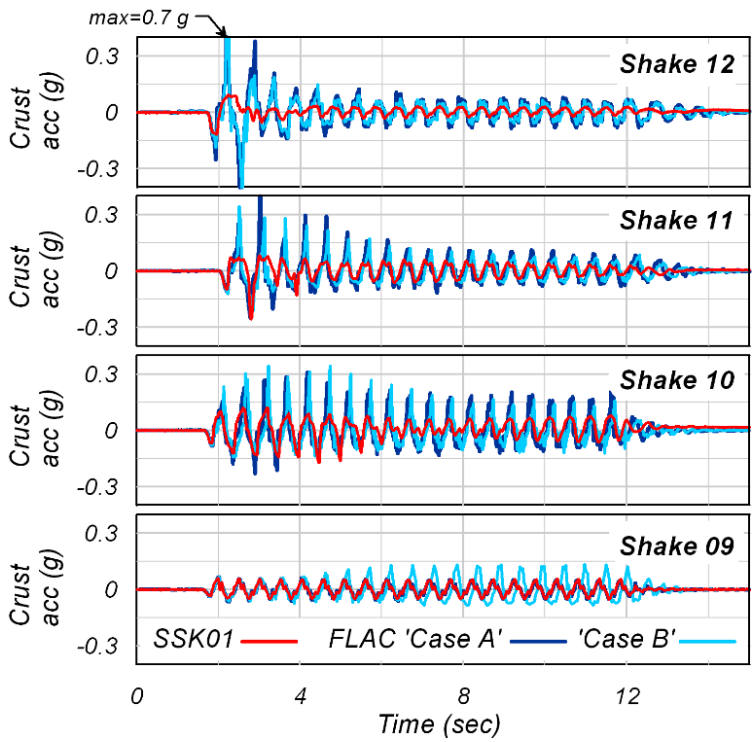

Figure 9. Crust acceleration on the non-treated side for all four shakes. Comparison of the centrifuge test (SSK01) with simulations using *'Case A'* and *'Case B'* cyclic strength values. (Kamai and Boulanger 2013)

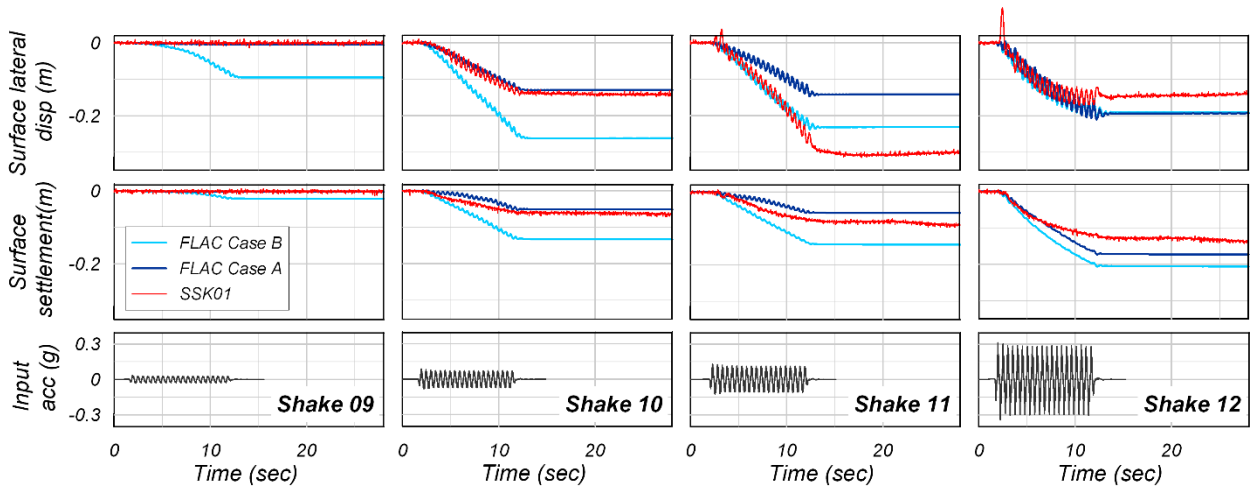

Figure 10. Displacement time histories on the non-treated side, shown for all four shakes. Comparison of the centrifuge test (SSK01) with simulations using *'Case A'* and *'Case B'* cyclic strength values. (Kamai and Boulanger 2013)

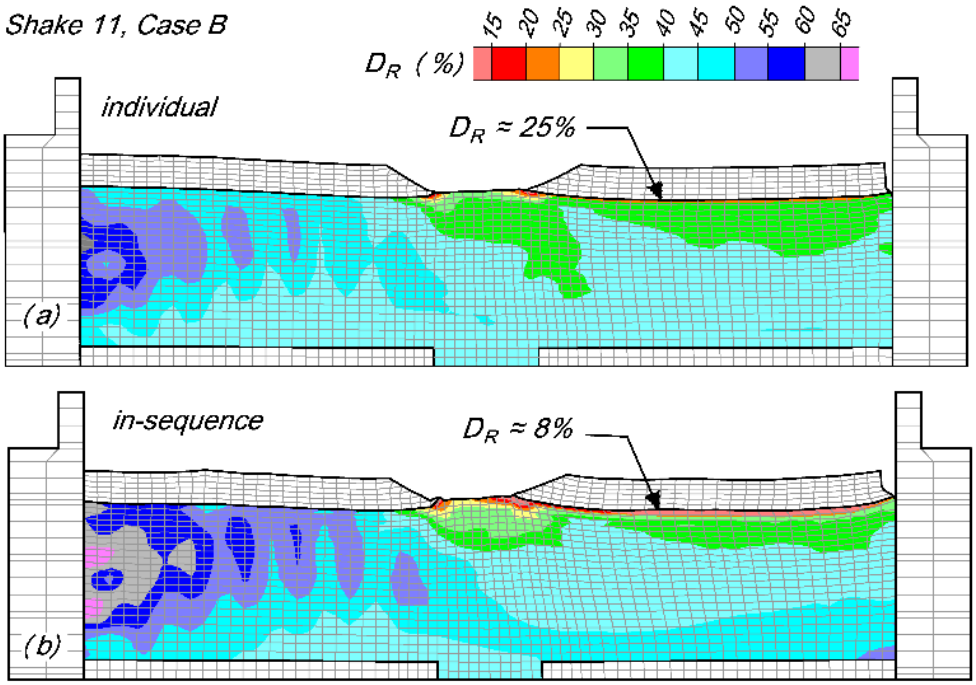

Figure 11. Contour plot of relative density (D_R) at the end of shaking, for the (a) individual and (b) in-sequence simulations of shake 11 with the *'Case B'* cyclic strength. (Kamai and Boulanger 2013)

Figure 12. Examples of localizations observed between the liquefied sand and overlying clay crust in models involving liquefaction-induced lateral spreading (Kamai 2011)

3.2 Submerged sand slope with embedded silt seams

The second set of simulations, which are reported in Kamai (2011) and Boulanger et al. (2013, 2014), was for a centrifuge model which consisted of a submerged slope of sand with an embedded silt arc and two embedded horizontal silt planes (Malvick et al. 2008), as shown in Figure 13. The model was subjected to two shaking events, each being of long-duration. Post-shaking photographs (e.g., upper photo in Figure 13) show that deformations were localized in a thin shear band at the silt-sand interface.

Simulations were performed using the finite different mesh shown in Figure 14 with the PM4Sand model and a baseline set of properties, followed by a sensitivity study covering a range of cyclic strengths, hydraulic conductivities, mesh size, and other parameters. The numerical simulations captured the trends and magnitudes of the recorded accelerations and pore pressures during shaking reasonably well. The simulations were in reasonable agreement with the final deformed geometry, but did not reproduce the delayed timing of the post-shaking slope deformations that were observed in the experiment. Details of the numerical modeling procedures and comparisons of the simulations with recordings are given in Kamai (2011).

The sand elements immediately below the silt arc in this mesh were generally about 200 mm thick, which is comparable to the expected dimensions of a potential shear band in this model. The median particle size for this sand is about 0.17 mm (model scale), such that a 10 to 20 grain diameter thick shear band would be 2 to 4 mm thick in model scale and thus 90 to 180 mm thick in the prototype scale used for the simulations. Analyses were also performed using a slightly more refined mesh, with the differences in results being consistent with those discussed previously. Considering the approximations involved in estimating the thickness of the localization zone, the values of the strains within the localized shear zone computed using the mesh in Figure 14 are expected to be reasonable for illustrating the mechanism of void redistribution.

Computed patterns of void redistribution for this model are illustrated by the results in Figure 15 for two different values of sand permeability. These more recent simulations were also performed using version 2 of the PM4Sand model (Boulanger and Ziotopoulou 2012), whereas the analyses in Kamai (2011) were performed using Version 1 (Boulanger 2010). The sand permeability for the case shown in Figure 15a was set equal to the value obtained in laboratory element tests, whereas the sand permeability was increased by a factor of five for the case shown in Figure 15b. This variation of permeability was chosen in part because some studies have suggested permeability increases markedly when liquefaction is

triggered (e.g., Haigh et al. 2012) and partly to examine the sensitivity of analysis results to the uncertainty in input parameters. These two numerical simulations produce patterns of void redistribution that are consistent with the patterns identified through back-analyses of the data from the dense array of pore pressure transducers (see Boulanger et al. 2014). The simulation results are consistent in showing that there is an approximately 1.0 to 3.0 m thick zone (varies along the arc) of sand immediately beneath the silt arc that loosens as a consequence of a net inflow of pore water, and that the greatest degree of loosening occurs in a thin zone immediately beneath the silt arc. For the case shown in Figure 15a, the sand elements immediately beneath the silt arc near the middle of the slope loosen from D_R = 35% before shaking to $D_R \approx$ 29% at the end of shaking and then to $D_R \approx$ 24.5% about 300 seconds after the end of shaking. For the case shown in Figure 15b, the same sand elements loosen more rapidly until they reach critical state at $D_R \approx$ 18% just before the end of shaking; these elements do not experience significant changes in D_R after shaking for this case, since most of the excess pore pressure dissipates during shaking due to the higher permeability. Thus, the five-fold increase in permeability between the models in Figures 15a and 15b increased the volumetric strains from about 2.2% to 3.6% at this point in the slope, caused a greater proportion of the strains to occur during shaking versus after shaking, and also increased overall slope deformations by about 18%. These effects are consistent with the simpler analytical and dimensional analysis results obtained by Kulasingam (2003).

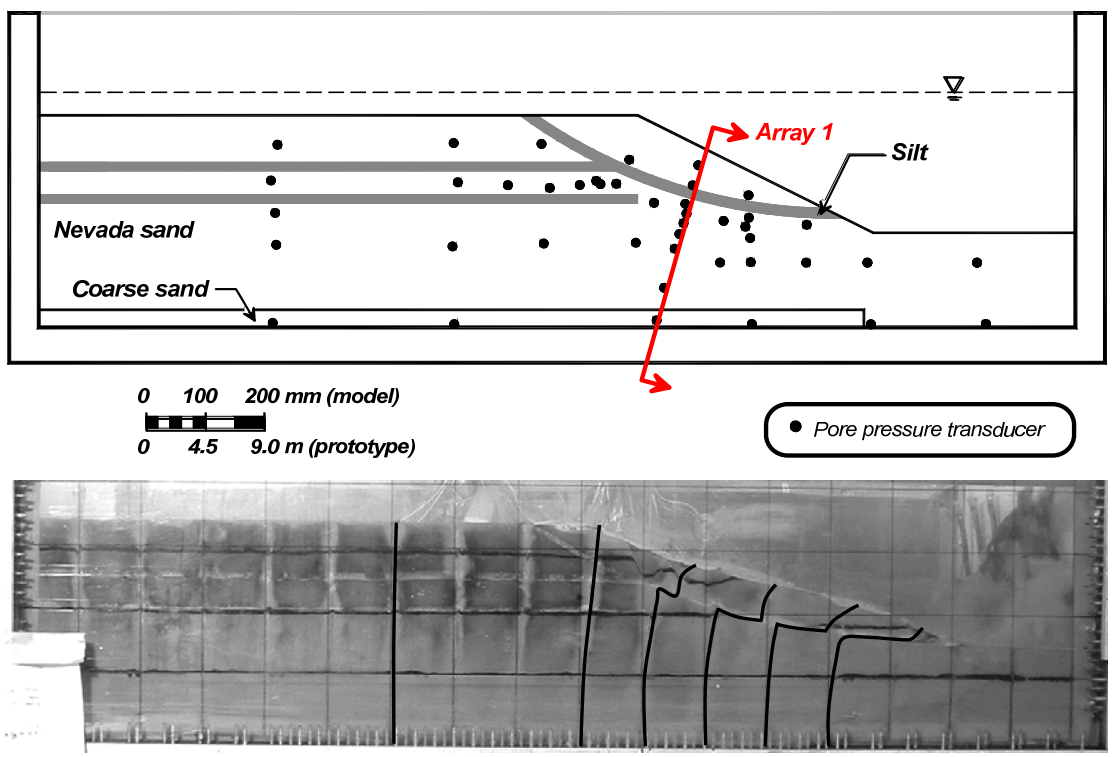

Figure 13. Localization of shear deformations along a lower permeability interlayer within a saturated sand slope tested in a 9-m-radius centrifuge (after Malvick et al. 2008)

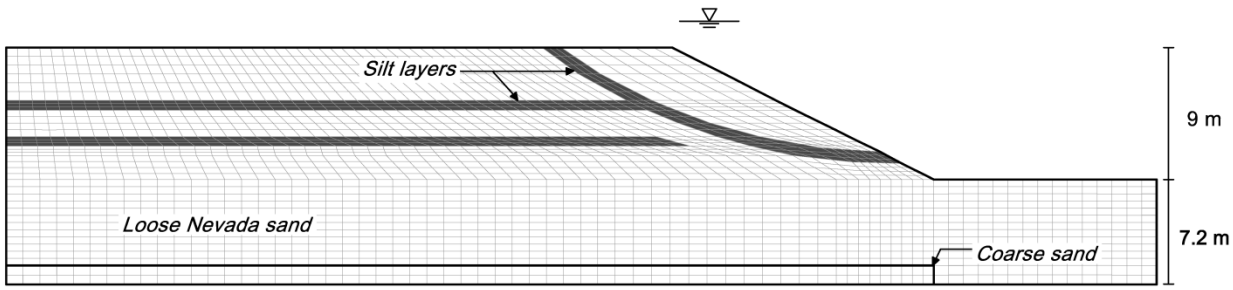

Figure 14. Model configuration and finite difference mesh for EJM02 (Boulanger et al. 2014).

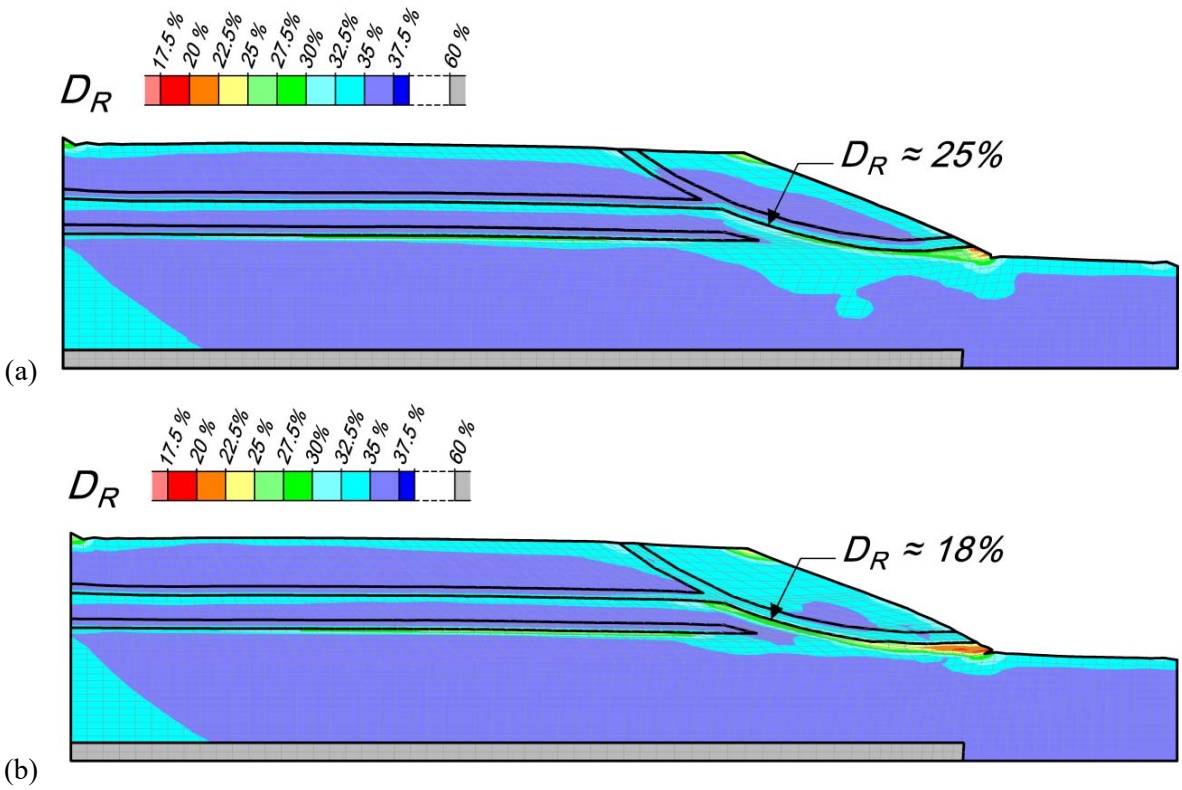

Figure 15. Deformed mesh and contours of D_R for two analysis cases that both start with an initial D_R = 35%: (a) sand permeability of 0.012 cm/s, and (b) sand permeability of 0.06 cm/s. (Boulanger et al. 2014)

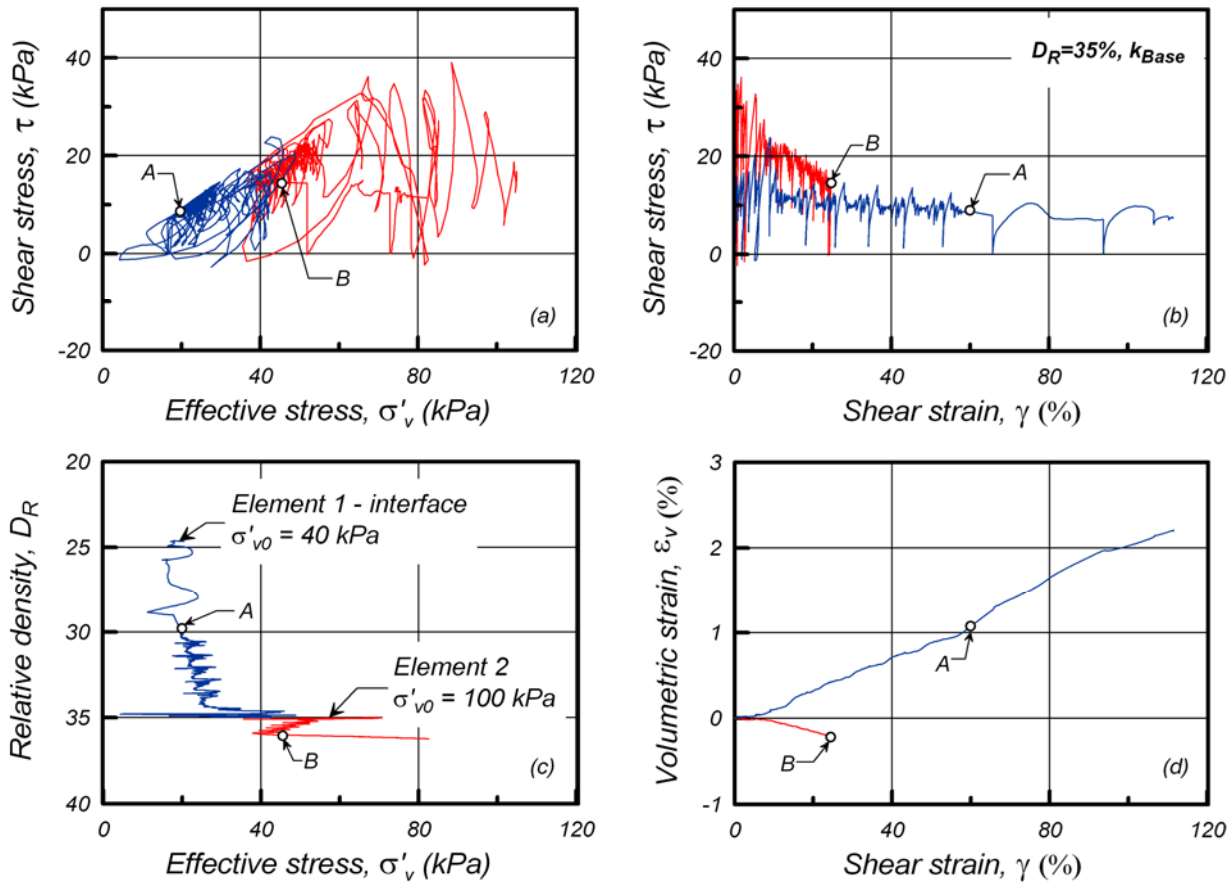

Figure 16. Stress and strain paths of two elements from one scenario simulation: Element 1 is in the sand just beneath the silt interlayer and Element 2 is about 6 m below Element 1. Points A and B represent the end of shaking for Elements1 and 2, respectively. (Boulanger et al. 2014)

The stresses and strains that were computed for two elements in the mesh for the simulation with the lower sand permeability are shown in Figure 16. Element 1 is a sand element just beneath the silt arc near the middle of the slope, whereas Element 2 is a few meters below Element 1 (below the zone of dilation). Points A and B correspond to the end of shaking for Elements 1 and 2, respectively. The sand at Element 2 developed high excess pore pressures and shear strains of several percent during shaking, but then progressively contracted (densified) due to the net outflow of pore water from this zone both during and after shaking. The sand at Element 1 also develops high excess pore pressures during shaking, but it progressively loosens under the net inflow of pore water and accordingly develops very large shear strains under the combined effects of this pore water inflow and continued small levels of shaking. The simulation paths are very consistent with the expected patterns described by Kulasingam et al. (2004).

4. Residual Strengths in Design and Evaluation

Engineering practice often requires that estimates be made for the residual shear strength of liquefiable soils that are denser than those represented in the flow slide case history database. For many practical problems, the potential failure plane for a slide mass may cut across materials with a range of $(N_1)_{60}$ values, such that the analysis of post-earthquake stability requires that estimates be made for the residual

shear resistance for all liquefiable zones (e.g., Figure 17). Since the case history database of flow slides only contains cases with $(N_1)_{60}$ values less than about 14 (e.g., Olson and Stark 2002), the estimation of residual strengths for liquefied soils with larger $(N_1)_{60}$ values involves extrapolation.

One challenge in extrapolating our empirical residual strength correlations is quantifying the effect that void redistribution may or may not have had on the in-situ residual shear strength for a given case history or field condition. The degree to which void redistribution may contribute to strength loss depends on numerous factors, as illustrated through the previously described physical model test results and numerical simulations. Case history-based relationships implicitly account for void-redistribution effects (Seed 1987), but the correlation of back-calculated residual shear strengths to pre-earthquake SPT blow counts or CPT penetration resistances does not provide a basis for differentiating between cases where void redistribution may or may not be significant. Equally important, the ability of our current nonlinear analysis procedures to reliably simulate the degree and extent of void redistribution for realistic geologic conditions has also not been demonstrated. Until we fully understand and can quantify the mechanisms of in-situ void redistribution and particle intermixing reasonably well, the risks associated with important structures dictate that we be cautious in our extrapolation of residual shear strength correlations.

In view of these practical challenges, Idriss and Boulanger (2007, 2008) proposed two possible scenarios for guiding the extrapolation of residual shear strength ratio (S_r/σ'_v) correlations to $(N_1)_{60}$ values greater than 14, as illustrated in Figure 18. The first scenario corresponds to conditions where the effects of void redistribution are expected to be negligible; e.g., the field conditions and stratigraphy are such that the post-earthquake pore water seepage will not be impeded by lower-permeability layers and thus the dissipation of excess pore pressures is expected to lead to densification of soils at all depths (in-situ void ratios decrease). In this case, the in-situ post-liquefaction shear resistance can be expected to be reasonably represented by relationships developed with consideration of laboratory element test results. This scenario provided guidance to the estimation of the upper curve, which bends strongly upward at $(N_1)_{60cs}$ values of 15-17, which Idriss and Boulanger (2007) recommended only for those cases where void redistribution effects are expected to be negligible.

The second scenario in Figure 18 corresponds to conditions where the effects of void redistribution can be significant; e.g., the field conditions and stratigraphy are such that the post-earthquake pore water seepage will, or could be, significantly impeded by an overlying lower-permeability layer. In this scenario, the potential for void redistribution-induced loosening and strength loss may be judged to represent a serious possibility. In such a situation, the potential increases in void ratio near an impeded drainage boundary would mean that relationships guided primarily by the results of laboratory element tests could significantly over-estimate the in-situ shearing resistance. For this scenario, Idriss and Boulanger (2007, 2008) recommended a lower relationship which curves more gently upward, eventually approaching drained strengths at an $(N_1)_{60cs}$ of about 32; this latter point on the residual strength curve was selected to agree with the limits of liquefaction triggering curves.

Nonlinear deformation analyses of geotechnical structures such as embankment dams often use case-history based correlations for estimating the in-situ residual shear-strengths of liquefied materials, but the way that the residual shear strengths are introduced to the numerical model depends on the constitutive model that is being used and certain engineering judgments. For example, the dynamic response analysis for an earthquake motion may be computed with the constitutive model first calibrated to produce a cyclic mobility response consistent with the pre-earthquake in-situ SPT or CPT penetration resistances. At the end of strong shaking, those elements which have exceeded some user-defined threshold (e.g., an excess pore pressure ratio or peak shear strain) may then be re-assigned a total stress constitutive model (e.g., Mohr Coulomb) having the desired value of residual shear strength. The analysis is then allowed to

progress forward in time to see if the drop to residual shear strengths results in an increase in post-shaking deformations (e.g., Naesgaard and Byrne 2007; Perlea and Beaty 2010). A thorough review of these and other practical aspects of evaluating liquefaction effects for embankment dams in practice is provided by Perlea and Beaty (2010).

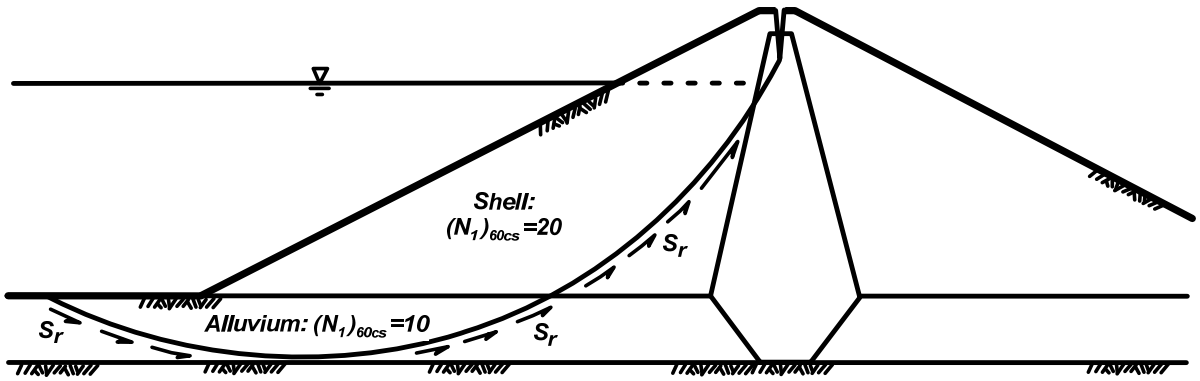

Figure 17. Schematic of an earth dam with two zones in which liquefaction may be triggered by strong earthquake shaking (Boulanger and Idriss 2011).

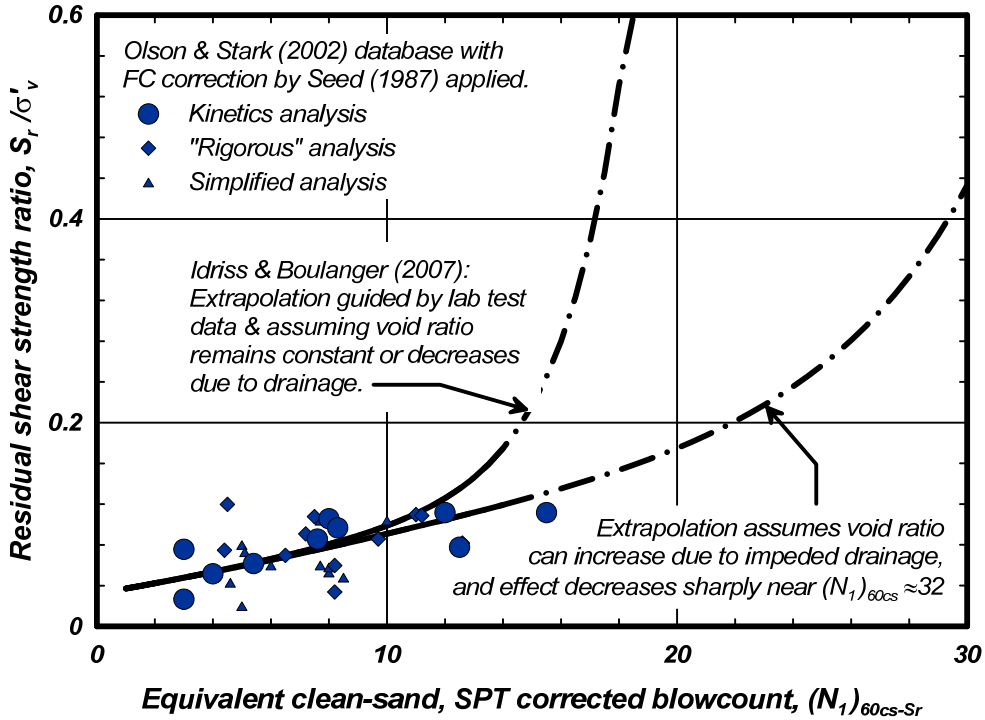

Figure 18. SPT-based correlation for cohesionless soils at σ'_{vc} < 400 kPa (Boulanger and Idriss 2011)

The practice of incorporating empirical residual shear strength correlations in post-shaking nonlinear deformation analyses was evaluated by Kamai (2011) as part of the simulations of the centrifuge model test shown in Figure 13. This approach produced deeper seated and larger than observed deformations, and did not capture the shear strain concentration observed at the silt-sand interface. These and other results suggest that the indirect procedure of using empirically-based residual shear strengths in these simulations cannot directly simulate the more localized effects of void redistribution. Nonetheless, this procedure remains a reasonable engineering approach for evaluating the potential consequences of void redistribution until more realistic analysis procedures have been proven effective.

5. Summary

The results of physical model tests involving liquefiable sands with lower-permeability interlayers have demonstrated how various factors can influence the degree to which void redistribution can affect shear strength losses and slope deformations. The potential for void redistribution to cause strain localizations and associated deformations in liquefied soil depends on the soil properties (initial relative density, cyclic resistance ratio, compressibility, permeability), slope geometry (layer thicknesses, slope angle, continuity of interfaces), and ground motion characteristics (shaking intensity, shaking duration, shaking history).

Numerical simulations using the critical-state compatible constitutive model PM4Sand (Boulanger and Ziotopoulou 2012) with the commercial program FLAC (Itasca 2011) were shown to reasonably reproduce the effects of partial drainage on elemental responses of liquefying sands (details in Kamai 2011 and Kamai and Boulanger 2012) and the patterns of void redistribution that were observed in two different centrifuge model tests (details in Kamai 2011, Boulanger and Kamai 2013, Boulanger et al. 2014). The numerical simulations provide additional insight on the mechanisms of void redistribution, although a number of factors that currently limit our ability to simulate void redistribution effects in practice were also identified.

The estimation of earthquake-induced deformations for geotechnical structures affected by liquefaction involves significant uncertainties, with the estimation of in-situ residual shear strengths being a major contributor to those uncertainties. It is hoped that an improved understanding of void redistribution effects will eventually lead to reduced uncertainties in estimating in-situ residual shear strengths and thus the performance of geotechnical structures.

Bibliography of publications resulting from the work

Boulanger, R. W., Kamai, R., and Ziotopoulou, K. (2014). "Liquefaction induced strength loss and deformation: Simulation and design." Bulletin of Earthquake Engineering, Springer, 12: 1107-1128, 10.1007/s10518-013-9549-x.

Kamai, R., and Boulanger, R. W. (2013). "Simulations of a centrifuge test with lateral spreading and void redistribution effects." Journal of Geotechnical and Geoenvironmental Engineering, ASCE, 139(8), 1250-1261.

Kamai, R. and Boulanger, R. W. (2012). "Single-element simulations of partial-drainage effects under monotonic and cyclic loading." Journal of Soil Dynamics and Earthquake Engineering, 35, 29-40.

Boulanger, R. W., Kamai, R., and Ziotopoulou, K. (2013). "Simulation of liquefaction-induced void redistribution in a centrifuge test." 10th International Conference on Urban Earthquake Engineering, March 1-2, Tokyo Institute of Technology, Tokyo, Japan, 301-305.

Boulanger, R. W., Kamai, R., and Ziotopoulou, K. (2011). "Numerical modeling of liquefaction effects." Proc., Effects of Surface Geology on Seismic Motion, 4th IASPEI / IAEE International Symposium, August 23-26, University of California, Santa Barbara, CA.

Kamai, R., and Boulanger, R. W. (2011). "Numerical simulations of a centrifuge test to study void-redistribution and shear localization effects." 8th International Conference on Urban Earthquake Engineering, Tokyo Institute of Technology, Tokyo, Japan, 455-459.

Kamai, R. (2011). Liquefaction-induced shear strain localization processes in layered soil profiles. Ph.D. dissertation, University of California, Davis.

Additional references cited in the report

Beaty, M., and P. M. Byrne (1998) "An effective stress model for predicting liquefaction behavior of sand," In: P. Dakoulas, M. Yegian, and R. Holtz, Eds., American Society of Civil Engineers, Geotechnical Special Publication, pp 766-777.

Boulanger, R. W. (2010). "Sand plasticity model for nonlinear seismic deformation analyses." Fifth International Conference on Recent Advances in Geotechnical Earthquake Engineering and Soil Dynamics, San Diego, CA, paper IMI-6.

Boulanger, R. W., and Idriss, I. M. (2011). "Cyclic failure and liquefaction: Current issues." Proc., 5th International Conference on Earthquake Geotechnical Engineering, Santiago, Chile.

Boulanger, R. W., and Ziotopoulou, K. (2013). "Formulation of a sand plasticity plane-strain model for earthquake engineering applications." Journal of Soil Dynamics and Earthquake Engineering, Elsevier, 53, 254-267.

Boulanger, R. W. and Ziotopoulou, K. (2012). PM4Sand (Version 2): A sand plasticity model for earthquake engineering applications. Report No. UCD/CGM-12-01, Center for Geotechnical Modeling, Department of Civil and Environmental Engineering, University of California, Davis, California, 100 pp.

Electric Power Research Institute (1993). Guidelines for site specific ground motions, Rept. TR-102293, 1-5, Pala Alto, California.

Haigh, S. K., Eadington, J., and Madabhushi, S. P. G. (2012). "Permeability and stiffness of sands at very low effective stresses." Geotechnique, 62(1), 69-75.

Idriss, I. M., and Boulanger, R. W. (2008). Soil liquefaction during earthquakes. Monograph MNO-12, Earthquake Engineering Research Institute, Oakland, CA, 261 pp

Idriss, I.M., and R. W. Boulanger (2007) "SPT- and CPT-based relationships for the residual shear strength of liquefied soils," In: K.D. Pitilakis, Ed., 4th International Conference on Earthquake Geotechnical Engineering - Invited Lecture. Athens: Springer, The Netherlands, pp 1-22.

Ishihara, K. (1996). Soil Behavior in Earthquake Geotechnics, The Oxford Engineering Science Series, No. 46.

Ishihara, K., and Yoshimine, M. (1992). "Evaluation of settlements in sand deposits following liquefaction during earthquakes." Soils and Foundations 32(1), 173–88.

Itasca (2009, 2011). *Flac - Fast Langrangian Analysis of Continua*, Version 6.0, Itasca Consultin Group, Inc., Minneapolis, Minnesota.

Kamai, R., and Boulanger, R. (2010) "Characterizing Localization Processes During Liquefaction Using Inverse Analyses of Instrumentation Arrays." In: Y.H. Hatzor, J. Sulem, and I. Vardoulakis, Eds., *Meso-Scale Shear Physics in Earthquake and Landslide Mechanics*. The Netherlands: CRC Press/.Balkema, pp 219-238.

Kokusho, T. (2003) "Current state of research on flow failure considering void redistribution in liquefied deposits," Soil Dynamics and Earthquake Engineering, Vol. 23, No. 7, pp 585-603.

Kulasingam, R. (2003). Effects of void redistribution on liquefaction-induced deformations. Ph.D. thesis, University of California, Davis.

Kulasingam, R., E. J. Malvick, R. W. Boulanger, and B. L. Kutter (2004) "Strength loss and localization of silt interlayers in slopes of liquefied sand," Journal of Geotechnical and Geoenvironmental Engineering, Vol. 130, No. 11, pp 1192-1202.

Malvick, E. J., B. L. Kutter, and R. W. Boulanger (2008) "Postshaking shear strain localization in a centrifuge model of a saturated sand slope," Journal of Geotechnical and Geoenvironmental Engineering, Vol. 134, No. 2, pp 164-174.

Malvick, E. J., B. L. Kutter, R. W. Boulanger, and R. Kulasingam (2006) "Shear localization due to liquefaction-induced void redistribution in a layered infinite slope," Journal of Geotechnical and Geoenvironmental Engineering, Vol. 132, No. 10, pp 1293-1303.

Naesgaard, E., P. M. Byrne, and M. Seid-Karbasi (2006) "Modeling Flow Liquefaction and Pore Water Redistribution Mechanisms," The 8th U.S. National Conference on Earthquake Engineering. San Francisco, California, USA.

Naesgaard, E., and Byrne, P. M. (2007). "Flow Liquefaction Simulation Using a Combined Effective Stress - Total Stress Model." 60th Canadian Geotechnical Conference, Canadian Geotechnical Society, Ottawa, Ontario.

NRC (1985) "Liquefaction of soils during earthquakes ". Washington, C.D.: National Academy Press.

Olson, S. M., and T. D. Stark (2002) "Liquefied strength ratio from liquefaction flow failure case histories," Canadian Geotechnical Journal, Vol. 39, No. 3, pp 629-647.

Perlea, V. G., and Beaty, M. H. (2010). "Corps of Engineers practice in the evaluation of seismic deformation of embankment dams." Fifth International Conference on Recent Advances in Geotechnical Earthquake Engineering and Soil Dynamics, San Diego, CA, paper SPL 6.

Seed, H. B. (1987) "Design-Problems in Soil Liquefaction," Journal of Geotechnical Engineering-ASCE, Vol. 113, No. 8, pp 827-845.

Seid-Karbasi, M., and P. M. Byrne (2007) "Seismic liquefaction, lateral spreading, and flow slides: a numerical investigation into void redistribution," Canadian Geotechnical Journal, Vol. 44, No. 7, pp 873-890.

Sento, N., Kazama, M., Uzuoka, R., Ohmura, H., and Ishimaru, M. (2004) "Possibility of Postliquefaction Flow Failure Due to Seepage." J. Geotechnical and Geoenvironmental Engineering, Vol. 130, No. 7, pp 707-716.

Vaid, Y.P., and A.A. Eliadorani, (1998). Instability and liquefaction of granular soils under undrained and partially drained states, Canadian Geotechnical Journal, 35 1053-1062.

Vaid, Y.P., and A.A. Eliadorani (2000). Undrained and drained (?) stress-strain response, Canadian Geotechnical Journal, 37 1126-1130.

Whitman, R.V. (1985) "On liquefaction," 11th International Conference on Soil Mechanics and Foundation Engineering. San Francisco, CA. Balkema Rotterdam, pp 1923-1926.